STRESS REDISTRIBUTION AROUND BROKEN FIBRES AND STRENGTH OF FIBRE BUNDLES

Luc St-Pierre, Silvestre Pinho

Department of Aeronautics, Imperial College London, London SW7 2AZ, UK
Email: l.st-pierre@imperial.ac.uk and silvestre.pinho@imperial.ac.uk
Web Page: http://wwwf.imperial.ac.uk/aeronautics/research/pinholab/

Keywords: Stress redistribution, Stress concentration factor, Strength of fibre bundles, Finite element analysis, Monte Carlo simulations

Abstract
Predicting the longitudinal tensile strength of composites requires accurate modelling of the stress redistribution that occurs around broken fibres. Recent work on this topic has focussed on the stress field surrounding a single broken fibre; however, this is an important limitation as unstable failure in carbon fibre bundles occurs when a cluster of about 16 or more broken fibres is formed. Therefore, we have developed a Finite Element (FE) model to investigate how stress redistribution varies with the number of broken fibres in a cluster. The results show that the stress concentration factor is sensitive to the size of the broken cluster; it increased from 1.06 for a single broken fibre to 1.17 for a cluster of 16 broken fibres. To ensure that these findings can be implemented effectively in fibre bundle models, we have also developed an analytical model that captures how the stress concentration factor varies with the number of broken fibres in a cluster, and validated its predictions against our FE simulations. Finally, we extended our FE model to predict the survival probability of fibre bundles using Monte Carlo simulations, and found that these predictions were in good agreement with experiments on microcomposites.

1. Introduction

The longitudinal tensile failure of composites is a complex process governed by: (i) variations in strength between each fibre and (ii) the stress redistribution that occurs around broken fibres. While strength variations can be quantified using single fibre tensile tests, insights on stress redistribution rely essentially on modelling efforts. Many early analytical models were developed to predict the stress field around multiple broken fibres [1–3], but these faced a number of limitations. First, only regular 1D [1] or 2D [2, 3] fibre packings can be represented. Second, the fibres and matrix were usually both modelled as linear elastic materials to simplify the analysis. Third, any solution to the problem would benefit of validation against robust direct numerical simulations.

These limitations were alleviated by the development of Finite Element (FE) models to study stress redistribution. This allowed to consider square [4], hexagonal [5, 6] and random [7] fibre arrangements, and to model the matrix as an elastic-plastic material [4, 6, 8]. However, FE studies conducted so far have analysed the stress redistribution that occurs around a single broken fibre, and this is an important restriction as there is growing experimental [9, 10] and analytical [11] evidence that unstable failure of a carbon fibre bundle occurs when a cluster of approximately 16 or more broken fibres is formed. Hence, there is a need to quantify how stress redistribution varies with the number of broken fibres, and this will be investigated in the first part of the paper using both analytical and FE modelling.

Excerpt from ISBN 978-3-00-053387-7

Representing accurately how stress redistribution varies with the size of the broken cluster is a critical part of models predicting the strength of fibre bundles, especially for those using a two-step simulation technique [8, 12–14]. With the latter approach, a deterministic model is first used to calculate the stress field around a single broken fibre. Second, a Monte Carlo simulation is performed in which fibres are assigned a stochastic strength and when a fibre breaks, the stress redistribution is done based on the solution obtained in the first step. A fundamental assumption of this technique is that stress redistribution around a cluster of broken fibres can be obtained simply by superposition of the stress field around a single broken fibre. Replacing this superposition method by a precise representation of how stress redistribution varies with the number of broken fibres should lead to more accurate strength predictions.

The two-step technique is not the only approach available to predict the strength of fibre bundles. Pimenta and Pinho [11] have developed an analytical model in which fibre bundles are assumed to be constructed hierarchically. Their predictions were in good agreement with experiments, but the effect of the hierarchical assumption on the results remains to be investigated. In contrast, other researchers have performed Monte Carlo FE simulations where (i) the fibres are interconnected by a network of shear springs representing the matrix [15, 16] or (ii) both the fibres and matrix are modelled with continuum elements [17]. The latter approach is computationally demanding; hence, limiting the analysis to very small volumes and making comparison with experiments difficult. Therefore, in the second part of this paper, we present computationally efficient Monte Carlo FE simulations, where the fibres are modelled with truss elements and the matrix is meshed with continuum elements. We first validate our approach by comparing our predictions to experiments on microcomposites. Then, our predictions are compared to the analytical model of Pimenta and Pinho [11] to analyse the effect of the hierarchical assumption.

This article is organised as follows. First, Section 2 focuses on the stress redistribution around clusters of broken fibres and contains: analytical predictions for the stress concentration factor; a description of the FE model developed and a comparison between analytical and FE predictions. Second, Section 3 presents the Monte Carlo FE simulations and includes a description of the modelling approach and a comparison between measured and predicted survival probabilities for two different microcomposites.

2. Stress concentration factor around a cluster of broken fibres

The fibre bundle considered to analyse stress redistribution is illustrated in Fig. 1a: it consists of a square arrangement of fibres and contains a cluster of broken fibres at its centre. All breaks are considered to be on the same plane, following recent x-ray tomographic observations which showed that 70% of clusters analysed had fibres broken in the same plane [14]. The bundle is loaded in tension by a remote tensile fibre stress σ^{∞}.

2.1. Analytical predictions

The problem of stress distribution is analysed here using polar coordinates, with the origin positioned at the centre of the broken bundle, see Fig. 1a. We define two equivalent radii, one for the entire bundle r_t and a second one for the broken cluster r_b, given as

$$\pi r_t^2 = n_t s^2 \Rightarrow r_t = \sqrt{\frac{n_t}{\pi}} s = \sqrt{\frac{n_t}{V_f}} \frac{\phi}{2} \quad \text{and} \quad \pi r_b^2 = n_b s^2 \Rightarrow r_b = \sqrt{\frac{n_b}{\pi}} s = \sqrt{\frac{n_b}{V_f}} \frac{\phi}{2}, \tag{1}$$

where n_t and n_b are the number of fibres in the bundle and in the broken cluster, respectively; ϕ is the fibre diameter; s is the fibre spacing and V_f is the fibre volume fraction. Before their failure, the broken fibres used to carry a total force

Excerpt from ISBN 978-3-00-053387-7

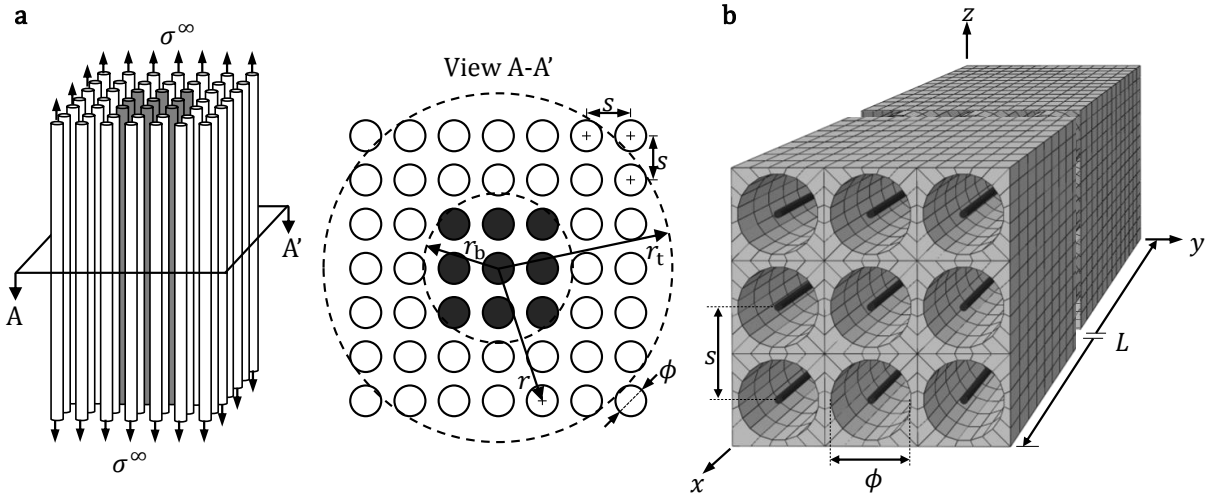

Figure 1. (a) Fibre bundle loaded in tension by a remote tensile stress σ^∞. The bundle contains, at its centre, a cluster of n_b broken fibres highlighted in grey. All breaks are coplanar and contained in the A-A' plane. The equivalent radii of the bundle r_t and of the broken cluster r_b are shown. (b) Finite Element model developed: the fibres, modelled with truss elements, are perfectly bonded to the matrix, meshed with continuum elements, using constraint equations.

$$\Delta F = \pi r_b^2 V_f \sigma^\infty, \tag{2}$$

which needs to be redistributed to unbroken fibres. To choose an appropriate stress redistribution profile, we first examine the solutions of similar problems. Consider a bar loaded in tension containing either a penny-shaped crack or a spherical cavity, both of radius a. For the penny-shaped crack, the tensile stress field scales as $\sqrt{a/r}$ [18], whereas for the spherical cavity it scales as $1 + A(a/r)^3 + B(a/r)^5$, where A and B are two constants [19]. Based on these two solutions, we anticipate that the stress redistribution around a cluster of broken fibres will take a similar power form: $(r_b/r)^\alpha$, where the value of the exponent α will be determined later. Hence, we hypothesise that the stress concentration factor can be written as

$$k = \frac{\sigma}{\sigma^\infty} = 1 + \lambda \left(\frac{r_b}{r}\right)^\alpha. \tag{3}$$

For a given value of α, the constant λ can be solved for by applying equilibrium:

$$\Delta F = \pi r_b^2 V_f \sigma^\infty = \int_{r_b}^{r_t} (\sigma - \sigma^\infty) V_f 2\pi r dr, \tag{4}$$

which gives

$$\lambda = \frac{1}{2\ln(r_t/r_b)} \quad \text{for } \alpha = 2 \quad \text{and} \quad \lambda = \frac{(2-\alpha) r_b^{2-\alpha}}{2(r_t^{2-\alpha} - r_b^{2-\alpha})} \quad \text{for } \alpha \neq 2. \tag{5}$$

Excerpt from ISBN 978-3-00-053387-7

Therefore, Eq. (3) can be used to predict the stress concentration factor k for a given value of α, which will be determined below from the FE results.

2.2. Description of Finite Element model

All computations to analyse the stress redistribution around a cluster of broken fibres were performed using the implicit solver of the commercially available FE code Abaqus (version 6.14). The fibre bundle considered had a length $L = 0.75\,\text{mm}$ and a fibre volume fraction $V_\text{f} = 60\,\%$. The bundle contained $n_\text{t} = 900$ carbon fibres, which had a diameter $\phi = 5\,\mu\text{m}$ and were squarely packed with a regular spacing $s = \sqrt{\pi/V_\text{f}}\phi/2 = 5.7\,\mu\text{m}$, as shown in Fig. 1b.

The fibres were discretised using 2-node linear truss elements (T3D2 in the Abaqus library), whereas the resin was meshed with 8-node linear brick elements with reduced integration and hourglass control (C3D8R in the Abaqus library). Constraint equations were used to represent a perfect bonding between the fibres and matrix. This approach of modelling the fibres with truss elements is more efficient than using continuum elements, and is consistent with experimental fibre strength characterisation which considers fibres to behave as one-dimensional entities. Both the fibres and matrix had a mesh size of $2\phi = 10\,\mu\text{m}$ along the fibre longitudinal direction. In the transverse direction, the matrix had a structured mesh with two elements between fibres, as shown in Fig. 1b. A convergence analysis revealed that further mesh refinement had a negligible effect on the results.

Only half of the bundle's length was modelled by applying symmetric boundary conditions at $x = 0$ and a prescribed displacement at $x = L$, see Fig. 1b. A square cluster containing $n_\text{b} = 1$ to 36 broken fibres was included at the centre of the bundle by removing the symmetric boundary conditions and the constraint equations at $x = 0$ for all broken fibres.

The material properties employed were chosen to represent the T800H/3631 carbon fibre prepreg and were obtained from Okabe and Takeda [20]. The T800H carbon fibres were modelled as a linear elastic material with a Young's modulus $E_\text{f} = 294\,\text{GPa}$. On the other hand, the 3631 epoxy was represented as an elastic-plastic solid: the isotropic elastic regime was characterised by a shear modulus $G_\text{m} = 1.2\,\text{GPa}$ and a Poisson's ratio $\nu_\text{m} = 0.40$, whereas the perfectly-plastic behaviour was in accordance with J2-flow theory and characterised by a shear yield strength $\tau_\text{y} = 52.4\,\text{MPa}$.

2.3. Results

Predictions of the stress redistribution that occurs in the plane containing the broken cluster are shown in Fig. 2a, where the relative increase in stress experienced by each unbroken fibre given by $k - 1 = (\sigma - \sigma^\infty)/\sigma^\infty$ is plotted as a function of the normalised distance r/s from the centre of the broken cluster (see Fig. 1a). Results are shown for different broken cluster sizes n_b and plotted on a logarithmic scale.

The results in Fig. 2a show that the increase in stress experienced by unbroken fibres is very sensitive to the number of broken fibres; the maximum value of $k - 1$ increases from 6% to 17% when the number of broken fibres increases from 1 to to the critical cluster size of 16. In addition, the stress profiles in Fig. 2a show that increasing the size of the broken cluster n_b increases not only the stress on the closest unbroken fibre but the entire stress distribution across the bundle.

The logarithmic scale used in Fig. 2a emphasises that, for a given value of n_b, $k - 1$ decreases linearly (on a log-log scale) with increasing r/s, where the slope corresponds to the value of the exponent α in Eq. (3). A slope of $\alpha = 2$ offers a good fit to the results shown in Fig. 2a. Now that the value of the exponent α is set to 2, we can compare the predictions of the analytical model presented in Section 2.1

Excerpt from ISBN 978-3-00-053387-7

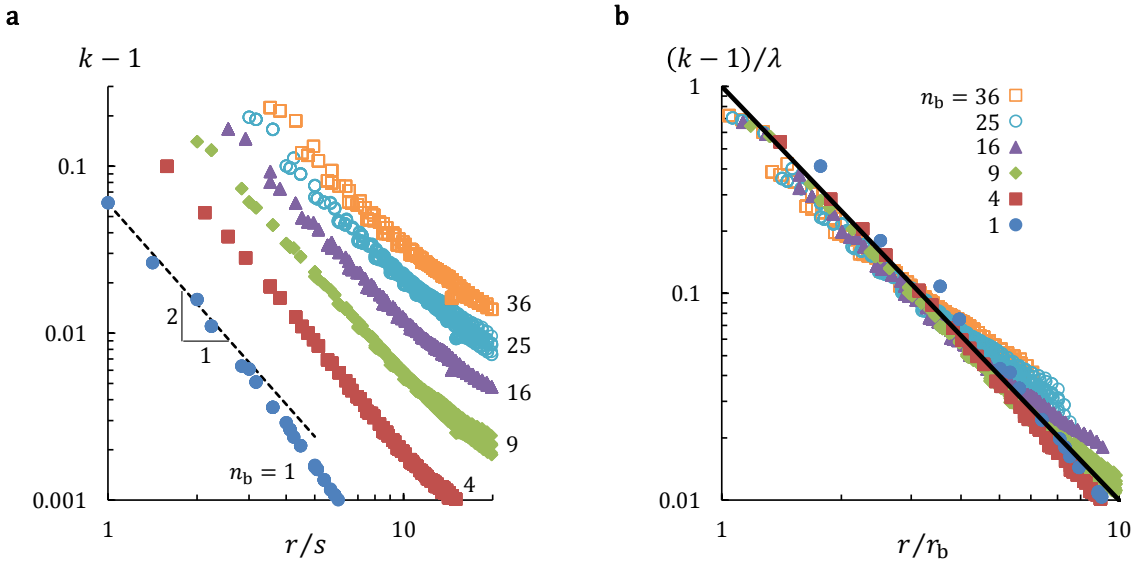

Figure 2. (a) Stress concentration factor k as a function of the normalised distance from the broken cluster r/s. (b) The same FE results are plotted with a different normalisation and compared to the predictions of Eq. (3). In both parts, results are shown for selected number of broken fibres n_b.

to the FE data shown in Fig. 2a. According to Eq. (3), all FE data should collapse on a single curve when plotted as $(k-1)/\lambda$ versus r/r_b. To test the accuracy of our analytical prediction, the data shown earlier in Fig. 2a is replotted using this normalisation in Fig. 2b. Clearly, there is an excellent agreement between the FE results and the analytical predictions over the entire stress distribution and for the wide range of n_b considered in this study. Hence, Eq. (3) offers an efficient and accurate prediction of the stress redistribution around clusters of broken fibres. Incorporating these findings in existing fibre bundle should lead to more accurate strength predictions.

3. Monte Carlo Finite Element predictions

3.1. Description of Finite Element model

The FE model described in Section 2.2 was modified to predict the survival probability of fibre bundles. These simulations are compared below to two different sets of experiments on microcomposites: the first set consists of four squarely packed AS4 carbon fibres in a blend of DER 331 and 732 epoxies (50:50) [21] whereas the second set has an hexagonal arrangement of seven IM6 carbon fibres embedded in a DER 331 epoxy [22].

The fibre bundles modelled had a length $L = 10$ mm, as used in the experiments [21, 22]. All degrees-of-freedom were constrained to zero at $x = 0$, whereas a prescribed displacement was applied at $x = L$, see Fig. 1b. The elements used and the mesh were the same as those described previously in Section 2.2.

The matrix was modelled as a linear elastic perfectly-plastic solid. In contrast, the fibres were modelled as linear elastic with failure (element deletion) when a maximum stress is reached. The strength of each fibre element σ_{el} was assigned to follow a Weibull distribution and scale according to weakest link theory such as

$$S_{el} = \exp\left[-\frac{L_{el}}{L_0}\left(\frac{\sigma_{el}}{\sigma_0}\right)^m\right] \quad \Rightarrow \quad \sigma_{el} = \sigma_0\left[-\frac{L_0}{L_{el}}\ln\left(S_{el}\right)\right]^{\frac{1}{m}}, \tag{6}$$

Excerpt from ISBN 978-3-00-053387-7

where L_{el} is the element length; the survival probability S_{el} is a randomly generated number; and σ_0 and m are the Weibull scale and shape parameters obtained from single fibre tensile tests at a gauge length L_0. All material properties employed are summarised in Table 1, and we emphasise that these were all obtained from experiments [21, 22].

All computations were performed in Abaqus using the dynamic implicit solver with the quasi-static option. To ensure convergence, the matrix included Raleigh material damping where $\alpha_m = 1.57e7\ s^{-1}$ and $\beta_m = 1.06e\text{-}4$ s are the mass and stiffness proportional factors, respectively. Numerical experimentation showed that these values of damping had a negligible effect on the results.

Table 1. Material properties employed in the Monte Carlo Finite Element simulations.

Fibre/Epoxy	Fibre properties						Matrix properties		
	ϕ (μm)	V_f	E_f (GPa)	σ_0 (GPa)	m	L_0 (mm)	G_m (MPa)	ν_m	τ_y (MPa)
AS4/DER 331+732	6.85	0.70	231	4.493	4.8	10	179.3	0.4	4.0
IM6/DER 331	5.63	0.56	280	5.283	5.4	10	604.5	0.4	46.6

3.2. Comparison with experiments

The survival probability of a bundle was obtained with 100 Monte Carlo FE simulations, and these predictions are compared to experiments on microcomposites in Fig. 3. Results are shown for a bundle with four AS4 fibres in part (a) and for one with seven IM6 fibres in part (b). The analytical predictions of Pimenta and Pinho [11] are also included for comparison.

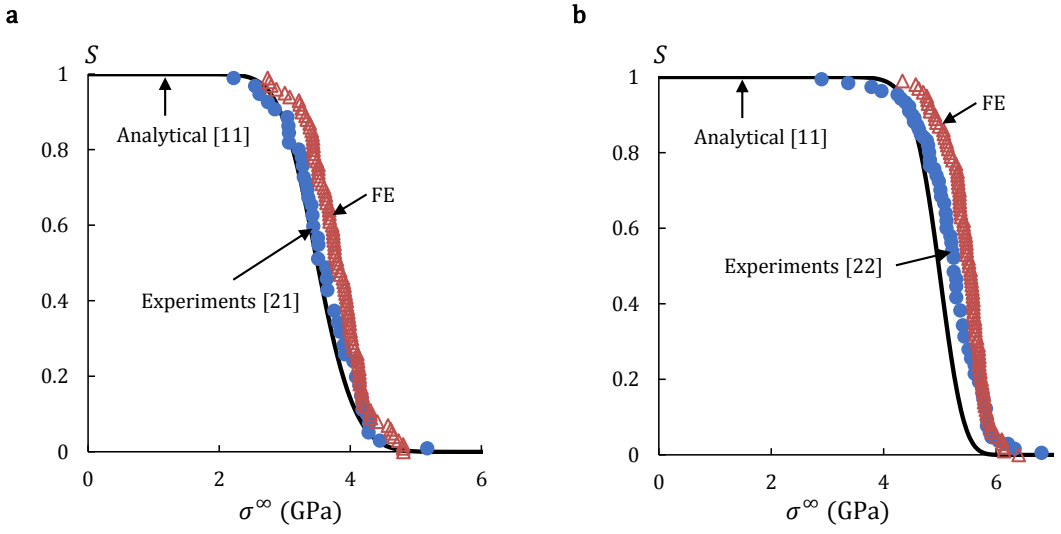

Figure 3. Survival probability S as a function of the remote tensile fibre stress σ^∞ for microcomposites with: (a) four AS4 carbon fibres in a blend of DER 331+732 epoxy (50:50) and (b) seven IM6 carbon fibres in a DER 331 epoxy. Monte Carlo Finite Element predictions are in good agreement with experimental [21, 22] and analytical [11] results.

Excerpt from ISBN 978-3-00-053387-7

In both cases, the the Monte Carlo FE simulations are slightly overestimating the measured survival probability, see Fig. 3. This could be due to the difficulty to measure accurately the constituent properties or the fact that fibre debonding is not included in the model. Nevertheless, the predictions are in good agreement with experiments, therefore validating our modelling approach. There is also a good agreement between the analytical and Monte Carlo FE predictions, which shows that the hierarchical assumption employed by Pimenta and Pinho [11] is valid for microcomposites.

4. Conclusion

Firstly, a Finite Element model was developed to investigate how stress redistribution in composites varies with the number of broken fibres in a cluster. The results showed that the stress concentration factor is very sensitive to the size of the broken cluster: the increase in stress in the fibre next to the broken cluster nearly tripled (from 6% to 17%) when the number of broken fibres was increased from 1 to the critical cluster size of 16. Analytical equations were also developed to predict how the stress concentration factor vary as a function of (i) the distance from the broken cluster and (ii) the number of broken fibres. These analytical predictions were found to be in excellent agreement with our Finite Element simulations for all broken cluster sizes considered. These findings can then be incorporated in fibre bundle models, which should lead to more accurate strength predictions.

Secondly, our Finite Element model was extended to predict the survival probability of fibre bundles using Monte Carlo simulations. The strength of each fibre element was assigned to follow a Weibull distribution obtained from single fibre tensile tests, and scale according to weakest link theory. The survival probabilities predicted by these Monte Carlo simulations were found to be in good agreement with experimental measurements and previous analytical results for two different microcomposites.

Acknowledgments

The authors are grateful for the financial support of the Engineering and Physical Sciences Research Council (EPSRC) under grant EP/M002500/1.

References

[1] J.M. Hedgepeth. Stress concentrations in filamentary structures. Technical Report NASA-TN-D-882, NASA Langley Research Center, Hampton, VA, May 1961.

[2] J.M. Hedgepeth and P. Van Dyke. Local stress concentrations in imperfect filamentary composite materials. *Journal of Composite Materials*, 1(3):294–309, 1967.

[3] J.G. Goree and R.S. Gross. Stresses in a three-dimensional unidirectional composite containing broken fibers. *Engineering Fracture Mechanics*, 13(2):395–405, 1980.

[4] B. Fiedler, A. Klisch, and K. Schulte. Stress concentrations in multiple fibre model composites. *Composites Part A*, 29(910):1013–1019, 1998.

[5] M.R. Nedele and M.R. Wisnom. Three-dimensional finite element analysis of the stress concentration at a single fibre break. *Composites Science and Technology*, 51(4):517–524, 1994.

[6] Z. Xia, T. Okabe, and W.A. Curtin. Shear-lag versus finite element models for stress transfer in fiber-reinforced composites. *Composites Science and Technology*, 62(9):1141–1149, 2002.

[7] Y. Swolfs, L. Gorbatikh, V. Romanov, S. Orlova, S.V. Lomov, and I. Verpoest. Stress concentrations

in an impregnated fibre bundle with random fibre packing. *Composites Science and Technology*, 74:113–120, 2013.

[8] Y. Swolfs, R.M. McMeeking, I. Verpoest, and L. Gorbatikh. Matrix cracks around fibre breaks and their effect on stress redistribution and failure development in unidirectional composites. *Composites Science and Technology*, 108:16–22, 2015.

[9] D.R.-B. Aroush, E. Maire, C. Gauthier, S. Youssef, P. Cloetens, and H.D. Wagner. A study of fracture of unidirectional composites using in situ high-resolution synchrotron x-ray microtomography. *Composites Science and Technology*, 66(10):1348–1353, 2006.

[10] A.E. Scott, M. Mavrogordato, P. Wright, I. Sinclair, and S.M. Spearing. In situ fibre fracture measurement in carbon-epoxy laminates using high resolution computed tomography. *Composites Science and Technology*, 71(12):1471–1477, 2011.

[11] S. Pimenta and S.T. Pinho. Hierarchical scaling law for the strength of composite fibre bundles. *Journal of the Mechanics and Physics of Solids*, 61(6):1337–1356, 2013.

[12] I.J. Beyerlein and S.L. Phoenix. Statistics of fracture for an elastic notched composite lamina containing weibull fibers part i. features from monte-carlo simulation. *Engineering Fracture Mechanics*, 57(23):241–265, 1997.

[13] W.A. Curtin and N. Takeda. Tensile strength of fiber-reinforced composites: I. model and effects of local fiber geometry. *Journal of Composite Materials*, 32(22):2042–2059, 1998.

[14] Y. Swolfs, H. Morton, A.E. Scott, L. Gorbatikh, P.A.S. Reed, I. Sinclair, S.M. Spearing, and I. Verpoest. Synchrotron radiation computed tomography for experimental validation of a tensile strength model for unidirectional fibre-reinforced composites. *Composites Part A*, 77:106–113, 2015.

[15] S.J. Zhou and W.A. Curtin. Failure of fiber composites: A lattice green function model. *Acta Metallurgica et Materialia*, 43(8):3093–3104, 1995.

[16] T. Okabe, N. Takeda, Y. Kamoshida, M. Shimizu, and W.A. Curtin. A 3d shear-lag model considering micro-damage and statistical strength prediction of unidirectional fiber-reinforced composites. *Composites Science and Technology*, 61(12):1773–1787, 2001.

[17] R.P. Tavares, A.R. Melro, M.A. Bessa, A. Turon, W.K. Liu, and P.P. Camanho. Mechanics of hybrid polymer composites: analytical and computational study. *Computational Mechanics*, 57(3):405–421, 2016.

[18] I.N. Sneddon. The distribution of stress in the neighbourhood of a crack in an elastic solid. *Proceedings of the Royal Society A*, 187(1009):229–260, 1946.

[19] S. Timoshenko and J.N. Goodier. *Theory of elasticity*. McGraw-Hill, 2 edition, 1951.

[20] T. Okabe and N. Takeda. Size effect on tensile strength of unidirectional cfrp composites: experiment and simulation. *Composites Science and Technology*, 62(15):2053–2064, 2002.

[21] I.J. Beyerlein and S.L. Phoenix. Statistics for the strength and size effects of microcomposites with four carbon fibers in epoxy resin. *Composites Science and Technology*, 56(1):75–92, 1996.

[22] M. Kazanci. Carbon fiber reinforced microcomposites in two different epoxies. *Polymer Testing*, 23(7):747–753, 2004.

Excerpt from ISBN 978-3-00-053387-7